DESIGN AND CONSTRUCTION OF EDDY CURRENT SENSORS WITH RECTANGULAR PLANAR COILS

J. Fava[1], A. E. Obrutsky, M. Ruch[1]
[1]CNEA; San Martin; Buenos Aires; Argentina.

Abstract: Eddy current sensors with rectangular planar coils were designed, constructed and characterized. The rectangular planar coils have a maximum testing area of 2.25 cm^2 and an output impedance in the range of the entrance impedance of normal commercial equipment (5 to 200 Ohm).
Two out of eight different windings have been studied so far, their electrical properties have been measured and calculated. In the characterization, sensor performance for three different eddy current applications has been checked, namely detection of surface and edge cracks and material sorting through resistivity assessment. The results were compared to those from a standard cylindrical probe.
A frequency range between (0.3–2.0) MHz was selected for crack inspection . Special testing pieces were prepared from Zircaloy-4 blocks. Crack signal analysis showed good amplitude discrimination and rather poor phase discrimination.
To test the resistivity response, a resistivity standard box and a Zircaloy-4 sample were used. The best operation points for this particular application corresponded to frequencies in the range (0.5–1.0) MHz.
The probes' strong points are: 1) the elimination of end effect in the inspection of edge cracks, 2) their good performance in the resistivity measurement at high frequencies, 3) their great sensitivity to detect crazes and other shallow imperfections, 4) the fact that any number of identical planar coils can be made from a single cliché.
The probes' weak points are: 1) low coil inductance values, 2) the construction of the probes: some probe stands might introduce unwanted signals.

Introduction: This work describes the design, construction and characterisation of eddy current sensors with rectangular planar spiral coils. Planar rectangular coils were first used at our laboratory in an inspection for edge cracks in cooperation with an NDT crew from abroad[1]. The main advantage of those rectangular planar coils was their power to eliminate (or at least minimise) the well known edge-effect, i.e., the characteristic bridge unbalance signal which is produced when the sensor approaches the edge of the conductive test piece.
The use of planar coils for defect detection and material characterisation has been reported by many authors.
Yamada et al. describe the construction of a special planar coil system for eddy current testing[2]. In another paper[3] the use of this system for crack detection in flat components is reported. Yamada et al. also use this system in the inspection for discontinuities in the circuit traces of printed circuits[4]. Many other authors have also constructed planar inductors and studied their properties[5-7]. Planar coils have been used for the assessment of electrical and magnetic properties of materials[8] and for the evaluation of thin resistive or magnetic layers on components[9]. On the other hand, our group has been involved in the e.t. assessment of electrical conductivity and oxide layer thickness using standard pancake coils [10-12].
In the present case, a simple mathematical model was the guideline for the design of the planar coils[13]. This model should provide a fast theoretical estimate of the electrical characteristics of the coils, i.e., if they might be used with currently available commercial ECT equipment. With this simple semiempirical model, coil impedances can be calculated but not the electromagnetic fields they generate. The values of the parameters thus calculated were directly used for coil design.

Two design criteria were adopted: coil sensitive area should be less than 2.25 cm^2 and its impedance should lie in the range (5 – 200) Ohm, i.e., the normal input impedance of commercial e.t. equipment. The coils were made at a company specialised in printed circuit manufacturing.
The present work is organized as follows: The first part describes the simple model used to determine coil design parameters as well as their actual physical characteristics and dimensions. The second part is devoted to the tests made to the coils and with the assembled sensors in order to establish their performance in two normal testing problems, namely crack detection and material sorting. It is also include a brief description of the test blocks especially designed and constructed for this task.

Results: 1 – Simple model for coil impedance evaluation: For the calculation of coil impedance in air, all three electrical parameters, inductance (L_0), resistance (R) and capacity (C) must be considered, as well as the operating frequency.
The resistance was calculated as $R=\rho l/s$, with l the length, s the cross section of the conductive traces and ρ, the resistivity of electrolytic copper, the material used in printed circuits. Coil capacity was estimated considering any pair of opposite traces (either on the same face of the fibre glass substrate or on opposite faces of it) as a pair of finite length wires separated by a dielectric. A relative dielectric constant of 4 was assumed for the fibre glass (tabulated values lie in the range 3-5) [14] whereas a value of 3.6 was assumed for the epoxi resin[14].
Previous experience in similar e.t. tests helped us fix the high frequency limit of the operating range at 2.0 MHz. A low frequency limit of 0.4 MHz was prompted by coil design itself, i.e., their low inductance and the 5 Ohm limit of the equipment.
A simple semiempirical approximation was used for the estimation of coil inductance, the most important and difficult calculation. It is based upon a theoretical expression for the calculation of the inductance of planar circular spiral coils[15] and considers a equivalent area approximation, which would enable the application of this model to our planar rectangular spiral coils. Hurley and Duffy[15] derive a formula for the calculation of the mutual inductance in air of two current carrying rings with radii r_1, r_2 and a_1, a_2, widths w_1, w_2 and thicknesses h_1, h_2, lying on parallel planes separated a vertical distance z. This model together with a equivalent area approximation was employed in the inductances calculation of our rectangular planar coils.
The calculated L_0, R and C values and those measured on our coils are presented in Table 1, $L_{0\text{-}Calc}$ standing for the $L_{0\text{-}Rect}$ discussed above. Tables 2 and 3 summarize the calculated and the measured impedances at the upper and lower operating frequencies. In these tables Z_{Calc} stand for the values calculated with the model, Z_{Med} are the impedances calculated from the L_0, R and C individually measured on our coils and $Z_{Med\ HP}$ denote the impedances directly measured with a HP4193A impedance meter from Hewlett Packard™.
Table 1. The calculated L_0, R and C values and those measured on our coils. The values denoted $L_{0\text{-}Calc}$ are the same as the $L_{0\text{-}Rect}$ in Eq. 2.

	Coil 1	**Coil 2**
Turns	2 x 10	2 x 7
$L_{0\text{-}Calc}$ (μHy)	3.1 ± 0.5	1.8 ± 0.3
$L_{0\text{-}Med}$ (μHy)	3.38 ± 0.03	1.58 ± 0.02
R_{Calc} (Ohm)	1.4 ± 0.1	1.2 ± 0.1
R_{Med} (Ohm)	1.25 ± 0.05	0.91 ± 0.05
C_{Calc} (pF)	31 ± 1	24 ± 1
C_{Med} (pF)	25 ± 1	17 ± 1

Table 2. Calculated and measured impedances of two-layer coil 1at the upper and lower operating frequencies.

Freq (kHz)	**Coil 1 – two layer design**		
	Calc	***Med***	***Med $_{HP}$***

	$\lvert Z_{Calc} \rvert$ (Ohm)	$\theta_{Z\text{-}Calc}$ (°)	$\lvert Z_{Med} \rvert$ (Ohm)	$\theta_{Z\text{-}Med}$ (°)	$\lvert Z_{Med\ HP} \rvert$ (Ohm)	$\theta_{Z\text{-}Med\ HP}$ (°)
400	7.8 ± 1.2	79.68 ± 0.03	8.59 ± 0.08	79.33 ± 0.02	9.78 ± 0.01	77.6 ± 0.1
2000	39.1 ± 6.2	87.89 ± 0.01	43.1 ± 0.3	87.81 ± 0.01	47.4 ± 0.1	86.3 ± 0.1

Table 3. Calculated and measured impedances of single-layer coil 2 at the upper and lower operating frequencies.

Freq (kHz)	**Coil 2 – single layer design**					
	Calc		***Med***		***Med $_{HP}$***	
	$\lvert Z_{Calc} \rvert$ (Ohm)	$\theta_{Z\text{-}Calc}$ (°)	$\lvert Z_{Med} \rvert$ (Ohm)	$\theta_{Z\text{-}Med}$ (°)	$\lvert Z_{Med\ HP} \rvert$ (Ohm)	$\theta_{Z\text{-}Med\ HP}$ (°)
400	4.6 ±0.7	74.82 ± 0.05	4.07 ± 0.06	71.87 ± 0.03	4.69 ± 0.01	70.3 ± 0.1
2000	22.3 ± 0.3	86.87 ± 0.01	20.0 ± 0.3	86.24 ± 0.01	21.7 ± 0.1	84.8 ± 0.1

2 – Characterization and analysis of coil response: 2.1 – Test blocks: Slots simulating planar cracks were cut on these slabs by electrical discharge machining (EDM) using a 0.1 mm diameter copper wire. The opening of the slots was 0.13 - 0.14 mm wide.

Two different types of slots were used, namely surface and edge slots. Three test blocks were constructed. For the surface defects, two slabs (100 mm x 50 mm x 7mm) were used; two slots were cut on one of the bigger faces of each of them. The edge slots were constructed on a (130 mm x 40 mm x 7 mm) block. On each of the 7 mm X 130 mm faces, two slots were made by EDM. Slot characteristics are presented in Table 4.

Table 4. Slots' depths for both kinds of test blocks used in this work.

Surface			**Edge**
Depth (mm)	Δ_{depth} (mm)		**Depth** (mm)
0.176	0.232 - 0.176 = 0.056	0.380 – 0.232 = 0.148	0.152
0.232			0.258
0.380	0.420 – 0.380 = 0.040		0.352
0.420			0.470

2.2 – Surface defects: Many tests were made with both coils at different frequencies in the range (0.4 MHz – 2.0 MHz). Figure 1 illustrates signals from coils 1 and 2 at different inspection frequencies. The features of the signals were always similar to those in Figure 1. Good amplitude discrimination is observed among the signals from the different slots. In fact, signal amplitude analysis enables discrimination between the two deeper slots or between the two shallower slots, though the actual depth difference is extremely small (Table 4). On the other hand, phase discrimination is rather poor, not to say nearly non-existent for single-layer coil 2.

2.2 – Surface imperfections: The signals from circumferential tool marks on the surface of the blocks blurred coil 1 indication of the shallowest slot at operation frequencies below 700 kHz. Detection of this shallowest slot was actually not possible with coil 2 at any of the operating frequencies used. These observations are related to the very high sensitivity of our coils for the detection of surface discontinuities. The blocks had some marks, Figure 2, and we overlooked the effect this surface roughness could have on the signals. These tool marks are unevenly distributed on the surface of the blocks, and are closer to each other in the region between the slots. The roughness was detected by our sensors and produced an unbalance of the bridge, which masked the indications from the shallower slot and prompted the need for special data processing. Figure 2 shows the signals produced by these tool marks, the central part of these graphs corresponding to the central part of the blocks[13].

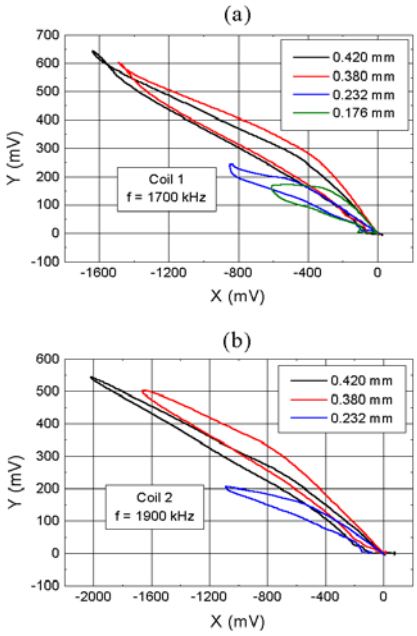

Figure 1. Signals obtained during the inspection of surface defects with two-layer coil 1 and single layer coil 2 at different inspection frequencies.

The inspection technique for edge defects requires bridge balancing with half of the coil area lying on the material and the other half on air as shown in Figure 4. Consequently, the depth of the slot is seen as a small cut. This is the balance condition for components which are to be tested for this kind of crack, if the surface to be inspected is not accessible, due to constructive or geometrical constraints. The probe stand used for this particular application is rather unstable and did not ensure a firm hold and uniform pressure throughout the inspection (we could not figure out so far how to include a spring or anything like it in the assembled probe). Some training of the inspector is therefore necessary before adequate signals are obtained.
The results from inspections with two-layer coil 1 at 1400 kHz are shown in Figure 3 (a). Figure 3 (b), perhaps one of the best results, was obtained with single-layer coil 2 at 800 kHz. As before, amplitude separation is very good while phase separation is rather poor.
Due to the test procedure that has been described, the low impedance of our probes can result in a poor signal to noise ratio. The cross section of the discontinuity, which effectively causes a distortion of the eddy currents, is in fact very small, far smaller than the cross section one would observe if the region which contains the crack opening. Special care must consequently be put in probe assembling, in order to minimise noise sources.

2.3 – Response for resistivity assessment and materials sorting: Two different tests were performed, the first one using materials covering the whole resistivity range of metals, the second one restricted to high resistivity materials. The former was made in order to study the general behaviour of our sensors, while the latter looked for their ability to discriminate among resistivity values which are very close to each other.

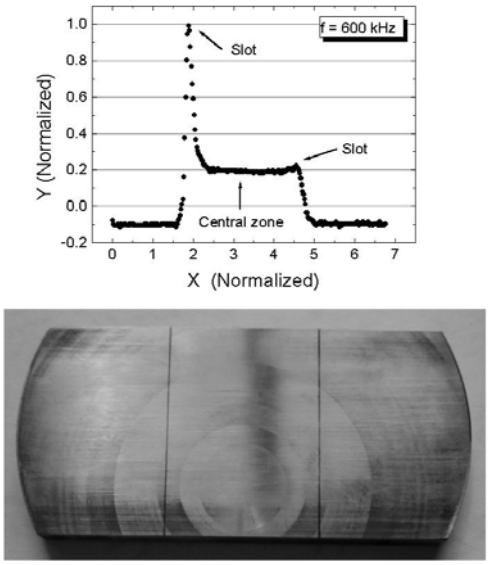

Figure 2. Tool marks on the surface of one of the Zircaloy-4 blocks used for the inspection of surface defects, and the x(t) component of one signal showing the unbalance of the bridge, which is a consequence of these surface imperfections.

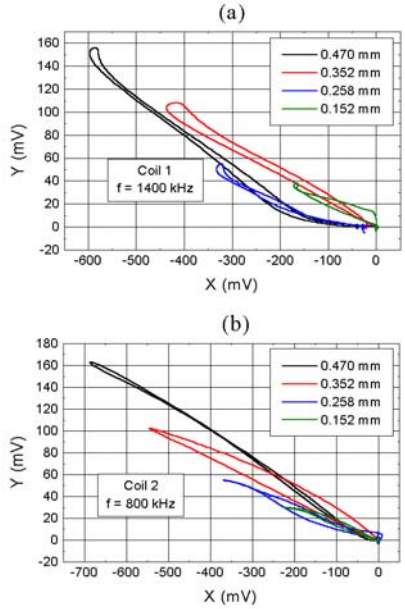

Figure 3. (a) Results from inspections of edge cracks with two-layer coil 1 at 1400 kHz of operation frequency, (b) results for single layer coil 2 at 800 kHz.

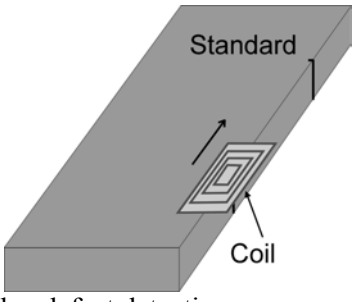

Figure 4. Balance technique for edge defect detection.

In the first case, the five materials of our resistivity standard set from Zetec (Table 5) and a Zircaloy-4 block were used, the resistivity of Zircaloy-4 is 70.0 μΩcm[13]. Figure 5 (a) shows the results of one of the tests on these set performed with two-layer coil 1, while one made with single-layer coil 2 is shown in figure 5 (b). In both cases the best results have been obtained at high frequencies, 300 kHz and 1.0 MHz. The largest angles between lift-off and the resistivity curve (nearly 90º) were obtained in this range as well as the best discrimination between high resistivity materials.

Table 5. Electrical resistivity of the five materials from the standard set from Zetec.

Material	Resistivity (μΩcm)
1	1.71
2	5.76
3	18.5
4	49.2
5	180.8

In the second case, the performance of these probes for the assessment of hydrogen content in Zircaloy[16,17] was tested. Three Zircaloy-4 specimens with different hydrogen content and a Zircaloy-4 sample in the as-received condition (see Table 6) were examined. The tests with two-layer coil 1 showed good separation among signals from the different specimens, as can be observed in Figure 6. These are in good agreement with those from Perotti and co-workers[12]. Single-layer coil 2 indications from the different specimens could not be discriminated, i.e. the separation of the points on the resistivity locus is less than the resolution of our equipment.

Table 6. Hydrogen content of the Zircaloy-4 specimens tested [12].

Sample	[H] (atomic %)
3C	4.9 ± 0.5
4C	7.3 ± 0.7
3B	12.1 ± 1

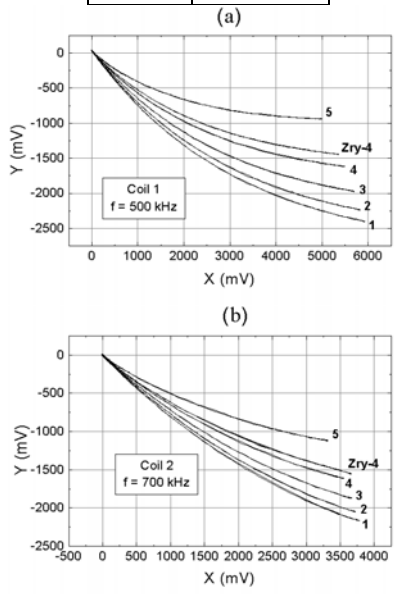

Figure 5. Material sorting tests on the resistivity standard set and the Zircaloy-4 block: (a) two-layer probe 1, (b) single-layer probe 2.

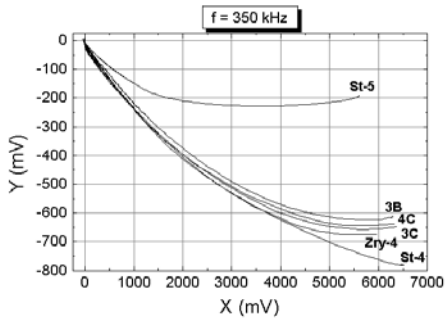

Figure 6. Resistivity assessments on the Zircaloy-4 samples with different hydrogen content and on as-received Zircaloy-4, two-layer coil 1.

Discussion: The general shape of the signals (for both coils and all types of slots) differs strongly from the curved signals normally obtained with circular pancake coils. Those obtained with the rectangular planar coils are rather straight and non symmetrical. The lack of symmetry could have been produced by the data processing we had to use in order to improve the signal to noise ratio prior to data analysis. The fact that the slope of the signal from the 0.380 mm slot is greater than that from the 0.420 mm slot calls our attention. This might be due to the surface condition of the blocks, because these particular slots are in different blocks with different tool marks.
A further analysis of the amplitude discrimination of these probes indicates that slots with depths differing in 0.04 mm can be separated, according to Table 4. It is likely that the detection limit of our probes was hampered by the indications from the surface imperfections of the slot blocks and the data processing that had to be used.
In the inspection for edge defects, probe performance was mainly limited by a poor stability of the coil stands, which prompted the need for a special type of data analysis and a better design.
A point which has not yet been addressed in the analysis of the coil response to surface slots is the fact that here too unwanted indications produced by the probe stands were observed, though these were far less important than those from surface imperfections or those reported in the test of edge slots. This also shows the high sensitivity of these coils to surface condition and to the coupling with the specimens.
Because $L_2 \approx \frac{1}{2} L_1$ it can be expected that the signals obtained with single-layer coil 2 be smaller than those from two-layer coil 1, and therefore the effect of surface imperfections and probe stands will result in a poor signal to noise ratio for coil 2.

Conclusion: Construction and characterisation of ect probes with planar coils was possible using a simple model for probe design.
Probe sensitivity for surface defect detection is very good, as can be deduced from the problems introduced by the tool marks. This fact indicates that the best probe stands for this kind of coils are those which ensure good coupling with the specimen, uniform pressure and minimum tilt among the components.
For defect detection, both two layer coil 1 and single layer coil 2 had very good amplitude discrimination and extremely low phase discrimination
Performance for material sorting was very good, mainly for coil 1. The best operation points are those for high frequencies (0.3 MHz a 1.0 MHz). These probes are specially suitable for characterisation of surface properties or thin layers. Coil 2 was not able to separate indications from specimens with different hydrogen content, thus showing that a 2 layer coil is more suitable for this problem than a single layer design.
The inductance can be increased by adding a high permeability substrate. However, a better way to achieve this should be by construction, i.e. to prepare new coils with a high density of narrower lanes and the use of multilayer design.

References: 1. J. Méndez, INEND-ENDE-CNEA, Private communication, 2002.
2. S. Yamada, M. Katoun, M. Iwahara and F. P. Dawson, 'Eddy Current Testing Probe Composed of Planar Coils', IEEE Trans. Magn., Vol. 31, No. 6, pp 3185-3187, Nov. 1995.
3. S. Yamada, M. Katoun, M. Iwahara and F. P. Dawson, 'Defect Images by Planar ECT Probe of Meander-Mesh Coils', IEEE Trans. Magn., Vol. 32, No. 5, pp 4956-4958, Sep. 1996.
4. S. Yamada, H. Fujiki, M. Iwahara, S. C. Mukhopadhyay and F. P. Dawson, 'Investigation of Printed Wiring Board Testing by Planar Coil Type ECT Probe', IEEE Trans. Magn., Vol. 33, No. 5, pp 3376-3378, Sep. 1997.
5. V. A. Franyuk and L. F. Ivan'kovich, 'Eddy-Current Transducer Based on Flat Spiral Coils', Institute of Applied Physics, Academy of Sciences of the Belorussian SSR., No. 4, pp 18-21, April 1988.
6. K. Kawabe, H. Koyama and K. Shirae, 'Planar Inductor', IEEE Trans. Magn., Vol. MAG-20, No. 5, pp 1804-1806, Sep. 1984.
7. M. Yamaguchi, M. Matsumoto, H. Ohzeki and K. I. Arai, 'Analysis of the Inductance and the Stray Capacitance of the Dry-Etched Micro Inductors', IEEE Trans. Magn., Vol. 27, No. 6, pp 5274-5276, Sep. 1991.
8. N.Ebine and K. Ara, 'Magnetic Measurement to Evaluate Material Properties of Ferromagnetic Structural Steels with Planar Coils', IEEE Trans. Magn., Vol. 35, No. 5, pp 3928-3930, Sep. 1999.
9. L. B. Pedersen, K. Å. Magnusson and Y. Zhengsheng, 'Eddy Current Testing of Thin Layers Using Co-planar Coils', Res. Nondestr. Eval., Vol. 12, No. 1, pp 53-64, 2000.
10. A. Lois, H. Mendonça and M. Ruch, 'Conductivity Calculations from Eddy Current Measurements on Thin Specimens', Insight, Vol. 44, No. 5, pp 279-283, May 2002.
11. C. C. Spinosa, 'Diseño, Construcción y Caracterización de un Sensor para la Medición de Espesores de Capas de Óxido sobre la Superficie Interna de los Canales de Combustible de la Central Nuclear de Atucha I', Tesis de Licenciatura en Ciencias Físicas, UBA, 1995.
12. A. Perotti, L. Lanzani, J.A. Marengo, M.Ruch, 'Non-destructive assessment of the thickness of oxide layers on Zircaloy-4: influence of hydrogen content', Insight, Vol. 42, No. 9, pp 597-602, September 2000.
13. J. Fava, 'Diseño y construcción de sondas para ensayos por corrientes inducidas conteniendo bobinas planas rectangulares', Tesis para optar al título de Magíster en Ciencia y Tecnología de Materiales, UNSAM-CNEA, 2003.
14. Dielectric constant reference guide, www.asiinstr.com/dc1.html, ASI Instruments Inc.
15. W. G. Hurley and M. C. Duffy, 'Calculation of Self and Mutual Impedances in Planar Magnetic Structures', IEEE Trans. Magn., Vol. 31, No. 4, pp 2416-2422, July 1995.
16. L. Lanzani and M. Ruch, 'Comments on the stability of zirconium hydride phases in Zircaloy', Journal of Nuclear Materials, Vol. 324, Issues 2-3, pp 165-176, January 2004.
17. A. Perotti, L. Lanzani, P. Coronel, M. Ruch, 'Preparation of calibration standards for eddy-current assessment of non-conductive coating thickness', Insight, Vol. 43, No. 5, pp 323-329, May 2001.